Journal of Materials Chemistry B

PAPER

CD133 antibody-conjugated immunoliposomes encapsulating gemcitabine for targeting glioblastoma stem cells

Cite this: *J. Mater. Chem. B*, 2014, **2**, 3771

Dae Hwan Shin, Shuhua Xuan, Woo-Young Kim, Gyu-Un Bae and Jin-Seok Kim*

Received 4th February 2014
Accepted 13th March 2014

DOI: 10.1039/c4tb00185k

www.rsc.org/MaterialsB

$CD133^+$ cells in glioblastoma multiforme (GBM) display glioma stem cell (GSC) properties and have been considered to be the culprit in tumor recurrence, justifying the exploration of potential therapeutic modalities targeting $CD133^+$ cells. Such strategies require a drug-delivery vehicle, and increasingly, the unique properties of PEGylated liposomes are being exploited for this purpose. More advanced liposomal delivery studies have suggested conjugation of CD133 antibodies as a suitable method for targeting GSCs. For targeting studies, GSCs separated from U87 GBM cells using a magnetic bead separation method were challenged with liposomes encapsulating gemcitabine (GEM) conjugated with a CD133 monoclonal antibody (PEG-lipo-CD133-GEM). An *in vitro* study showed that conjugation of CD133 antibody significantly enhanced the cytotoxicity of GEM through endocytosis of CD133 surface markers overexpressed on GSCs. The anti-tumor effect of PEG-lipo-CD133-GEM was 15 times higher than that of free GEM, presumably reflecting the specific targeting of the CD133 surface marker by PEG-lipo-CD133-GEM and the enhanced stability and cytotoxicity through the PEGylated liposome formulation in xenograft models. Moreover, monitoring of body weight changes showed that the use of PEGylated liposomes significantly reduced the toxicity of GEM. Taken together, our studies demonstrate that PEG-lipo-CD133-GEM shows promise for the treatment of gliomas *in vitro* and in xenograft models.

Introduction

Glioblastoma multiforme (GBM), the most frequent primary brain tumor, has aggressive and highly invasive properties. It is also highly lethal, with patients exhibiting a median survival time of about 1 year after the initial diagnosis.[1–3] Despite aggressive treatment with surgery, radiotherapy and chemotherapy, malignant GBM is associated with poor prognosis and remains difficult to eliminate.[4] GBMs present as diffuse tumors with invasion into normal brain tissue, but frequently recur or progress after radiation as focal masses, suggesting that only a fraction of cancer cells is responsible for regrowth. These cells are known as glioblastoma-initiating cells (GICs) or glioblastoma stem cells (GSCs).[5] Accumulating evidence also suggests that most malignant solid tumors may contain stem cells.[6–8]

The pentaspan transmembrane glycoprotein family member CD133, also known as prominin-1 (PROM-1), is expressed as several isoforms with unknown physiological or pathological functions that are specifically localized on cellular protrusions.[9,10] Despite some controversial findings, CD133 is the best-validated marker of the cell subpopulation responsible for conferring stem cell properties to GBMs.[11] Several studies have identified CD133 as a marker of GSCs, showing that only $CD133^+$ cells from brain tumor biopsy specimens are able to initiate brain tumors in an immunodeficient mouse model,[10] making CD133 an attractive target for delivery of targeting therapeutics. Recent reports have further shown that expression of the CD133 antigen in GBMs, medulloblastomas, and other brain cancers could serve as a prognostic indicator of tumor regrowth, malignant progression, and patient survival.[12,13] Although the roles of CD133 in GSCs are not fully characterized, recent data suggest that new therapeutic strategies designed to specifically target the $CD133^+$ (GSC) sub-population are necessary to more effectively eliminate malignant tumors and reduce the risk of relapse.[14,15]

Gemcitabine (2′,2′-difluorodeoxycytidine; trade name Gemzar, GEM) is a deoxycytidine analogue that plays a well-established role in treating several types of solid tumors and human tumor xenografts. It is a broad spectrum oncolytic compound indicated as a single agent for the treatment of metastatic pancreatic cancer and, in combination therapy, for the treatment of ovarian and breast cancer and non-small cell lung carcinoma.[16] The anti-cancer efficacy of GEM is currently being tested clinically against bladder cancer, colorectal cancer and cervical cancer.[17–19] Recent reports indicate that GEM-mediated toxicity can be transferred through gap junctions, suggesting that GEM treatment could be highly effective against solid tumors that display gap junctions, such as GBM and

Research Center for Cell Fate Control (RCCFC) & College of Pharmacy, Sookmyung Women's University, 53-12 Chungpa-2 Dong, Yongsan-Gu, Seoul 140-742, Korea. E-mail: jsk9574@sm.ac.kr; Fax: +82 2 710 0032; Tel: +82 2 710 9574

osteosarcoma, through the "bystander effect".[20,21] Prospective clinical results also suggest the effectiveness of combined treatment of GBM with GEM and radiation therapy.[22,23] However, GEM is associated with greater hematological toxicity and other side effects, and its therapeutic index is also insufficient because of its cytotoxicity to healthy normal cells.[24] Another limitation to GEM efficacy that is common to other chemotherapeutic agents is its poor penetration into solid tumors.[25,26]

It is well known that liposomes made from naturally occurring phospholipids are biocompatible carriers that, when used in drug delivery systems, can reduce the systemic toxicity of the drug and overcome resistance of traditional chemotherapeutics, thereby increasing the therapeutic efficacy.[27,28] Although rapid elimination by the reticuloendothelial system (RES) is recognized as one of the major drawbacks of conventional liposomes in anti-cancer drug delivery, this can be overcome by modifying liposomes with flexible hydrophilic polymers, such as polyethylene glycol (PEG).[29–31] It has been reported that PEGylated liposomes noticeably improved the growth-inhibitory activity of GEM in various cancer cells including pancreatic or myeloma cancer cells.[32,33] Liposomal delivery of GEM significantly increased the induction of apoptosis and caused a complete inhibition of proliferation of cancer cells.[32–34] Specific targeting of GSCs can be achieved by conjugating PEGylated liposomes with an antibody against CD133 which is overexpressed on GSCs.

In the current study, we have developed a therapeutic liposome formulation against GSCs, selecting GEM as the "payload". To reduce GEM cytotoxicity and improve its stability and the efficiency of its cellular uptake by GSCs, we selected PEGylated liposomes conjugated with an anti-CD133 monoclonal antibody (CD133-Ab). The use of CD133-Ab-conjugated, PEGylated liposomes as a drug-delivery carrier for GEM is also expected to enhance the *in vivo* stability and improve the pharmacokinetic properties and anti-cancer efficacy of GEM after systemic administration into the body. We show that GSCs were selectively targeted and suppressed *in vitro* and in xenograft models by CD133-Ab-conjugated PEGylated immunoliposomes encapsulating GEM (PEG-lipo-CD133-GEM). We suggest that PEG-lipo-CD133-GEM may form the basis of a novel therapeutic strategy for eliminating malignant tumors, such as GBMs, by specifically targeting GSCs.

Materials and methods

Chemical reagents and antibodies

GEM HCl, commercially known as Gemzar (Lilly, France), was purchased from Shinwon Pharmacy Co. (Seoul, Korea). Fluorescently (Cy5.5) labeled GEM, prepared by chemical modification of GEM, was obtained from Genechem Inc. (Daejeon, Korea). 1,2-Dipalmitoyl-*sn-glycero*-3-phosphocholine (DPPC), 1,2-distearoyl-*sn-glycero*-3-phosphoethanolamine-*N*-[methoxy-(polyethylene-glycol)-2000] (DSPE-mPEG$_{2000}$), and 1,2-distearoyl-*sn-glycero*-3-phosphoethanolamine-*N*-poly(ethylene-glycol)-2000-*N*-3-(2-(pyridyldithio)propionate) (DSPE-PEG-PDP) were purchased from Avanti Polar Lipids (Alabaster, AL, USA). The anti-CD133 monoclonal antibody was purchased from ABNOVA (Taipei, Taiwan). Ammonium sulfate, 3-(4,5-dimethylthiazol-2-yl)-2,5-diphenyl-2*H*-tetrazolium bromide (MTT), chloroform ($CHCl_3$), accutase, human epidermal growth factor (hEGF), fibroblast growth factor-basic (bFGF), cholesterol (Chol), dithiothreitol (DTT), and methanol (MeOH) were purchased from Sigma Chemical Co. (St. Louis, MO, USA). B-27 supplement (B27) was purchased from Invitrogen (Carlsbad, CA, USA). Dulbecco's Modified Eagle's Medium (DMEM), DMEM/F12, fetal bovine serum (FBS), trypsin–EDTA, Dulbecco's phosphate-buffered saline (DPBS), and penicillin/streptomycin were purchased from WelGENE Inc. (Daegu, Korea). All reagents and solvents were of analytical grade or better.

Sorting of GSCs from U87 cells using MACS technology

U87 GBM cells were obtained from the American Type Culture Collection (ATCC; Manassas, VA, USA) and were cultured as monolayers in DMEM containing 10% FBS and 100 U ml^{-1} penicillin/streptomycin at 37 °C in a humidified 5% CO_2 atmosphere. For growth as spheroids, U87 cells were resuspended in stem cell-permissive medium consisting of DMEM/F12 containing 20 ng ml^{-1} of hEGF, bFGF and B27 (1 : 50), as reported elsewhere.[35,36] Spheres were collected after 7 days and dissociated with accutase solution (Sigma Chemical Co., St. Louis, MO, USA). GSCs were sorted by magnetic-activated cell sorting (MACS) using a MACS separation kit (Miltenyi Biotec Ltd, Teterow, Germany) according to the manufacturer's instructions. Briefly, 1×10^8 cells per 300 μl were incubated with 100 μl CD133/1 magnetic bead solution and 100 μl FcR blocking buffer for 30 minutes on ice. CD133$^-$ and CD133$^+$ cells were then separated using the CD133 cell isolation kit. The efficiency of sorting was verified by fluorescence-activated cell sorting (FACS) and Western blot analyses. Only cell populations with greater than 90% CD133$^+$ cells were used as GSCs for experimentation.

Determination of CD133 expression in GSCs

CD133 expression in different cell populations was directly analyzed by Western blotting and quantified by FACS. In Western blot analysis, lysates of sorted (CD133$^-$ and CD133$^+$) and unsorted U87 cells were prepared by extracting proteins with lysis buffer (50 mM Tris–HCl pH 7.4, 150 mM NaCl, 0.1% Triton X-100) supplemented with protease inhibitors. Proteins were separated by sodium dodecyl sulfate-polyacrylamide gel electrophoresis (SDS-PAGE) and transferred to nitrocellulose membranes. The membranes were blocked with 5% non-fat, dry skim milk in Tris-buffered saline and then incubated with primary CD133-Ab overnight at 4 °C. The blots were developed with peroxidase-conjugated secondary antibody, and proteins were observed using enhanced chemiluminescence procedures (Supersignal® West pico chemiluminescent substrate; Thermo Scientific, IL, USA), according to the manufacturer's protocol. To more clearly identify the CD133 expression in GSCs, the efficiency of sorting was verified by flow cytometry using a phycoerythrin (PE)-conjugated-CD133/2 antibody (CD133-PE; Miltenyi Biotec). Sorted (CD133$^-$ and CD133$^+$) and unsorted

U87 cells were washed three times and fixed with 4% paraformaldehyde for 10 minutes. Appropriately diluted cells were stained with CD133-PE and analyzed with a FACSCanto II system (Becton Dickenson, San Jose, CA, USA), as described by the manufacturer.

Proliferation of GSCs in DMEM containing FBS

The cell growth of GSCs in DMEM containing 10% FBS was assessed using MTT-based proliferation assays. Sorted GSCs and unsorted U87 cells were seeded onto tissue culture plates and incubated for 24 hours to allow cells to adhere to the bottom of the plate. After the non-adherent cells and the culture medium were removed, the adherent cells were detached, dissociated into a single-cell suspension by accutase solution, and seeded into 48-well plates at 2×10^4 cells per well in DMEM containing 10% FBS. On days 1, 2, 3, 4, 5, 6, 7 and 8, the culture medium was removed and MTT solution (1 mg ml^{-1}) was added. The cells were incubated for 4 hours, after which the medium was replaced with 0.5 ml dimethyl sulfoxide (DMSO). The plates were agitated for 15 minutes and the optical density of the solution in the wells was measured at 570 nm using an ELISA reader (EL 800; BioTek, Winooski, VT, USA). Cells on day 0 were taken as the blank with 0% growth. Triplicate experiments were performed, and the values are presented as mean ± SD.

Chemoresistance of GSCs and unsorted U87 cells

To compare the chemoresistance of sorted GSCs and unsorted U87 cells, we tested the anticancer agent (GEM) using a MTT assay. The cells were seeded onto 48-well plates (2×10^4 cells per well) and treated with different concentrations of GEM. After incubating for 48 hours, the culture medium was removed and MTT assays were performed as described above. Untreated cells incubated for 48 hours were taken as control with 100% growth and cells without incubation were used as blank with 0% growth. Triplicate experiments were performed, and values are presented as mean ± SD. The 50% inhibitory concentration (IC_{50}) value was calculated using Sigmaplot version 10.0 software.

Tumor sphere formation assay

GSCs and unsorted U87 cells were dissociated and single cells seeded in 96-well plates in 0.1 ml per well of serum-free DMEM/F12 medium. Every 3 days, 0.02 ml medium were added to the culture. The percentage of the wells containing spheres with more than 50 cells was calculated on day 14 to examine the efficacy of clonogenesis. Unsorted parental U87 cells were used as controls for the capacity to form tumor cell clones. The secondary spheres derived from single cells were examined by microscopy.

Tumorigenic capacity of GSCs in BALB/c nude mice

All animal experiments were approved by the SMU-IACUC of the Sookmyung Women's University, Korea. Male, 6 week old, BALB/c nude mice were purchased from Jung-Ang Lab Inc. (Seoul, Korea). Xenografts were generated by injecting 1×10^6 sorted GSCs or unsorted U87 cells in 70 μl into the right flank. The mice were observed twice a week and sacrificed at the end of the experiment. Tumor size was determined twice weekly by measuring the two perpendicular dimensions using Vernier calipers (Mitutoyo Co., Kanagawa, Japan). Tumor volume was estimated using the following equation:

$$\text{Tumor volume } (\text{mm}^3) = \frac{1}{2}(\text{length} \times \text{width}^2) \quad (1)$$

Preparation of PEGylated liposomes for antibody conjugation

PEGylated liposomes composed of DPPC : Chol : DSPE-$mPEG_{2000}$: DSPE-PEG-PDP at a molar ratio of 2 : 1 : 0.08 : 0.02 were prepared and characterized as reported elsewhere.[34] Briefly, the lipid mixture (40 mM) was dissolved in a round-bottomed flask using a chloroform–methanol (3 : 1 v/v) solvent mixture, after which the solvent was removed using a rotary evaporator (Laborota-4000; Heidolph, Germany), leaving a thin-layer lipid film. The lipid film was hydrated with a 250 mM ammonium sulfate solution (2 ml) and then subjected to 10 cycles of freezing (liquid nitrogen) and thawing (40 °C water bath), thereby achieving a pH gradient such that intra-liposomal aqueous compartments possessed a homogenous acidic environment. Multilamellar vesicles were extruded through two stacked polycarbonate filters with pore sizes of 450 and 200 nm (Whatman, Schwerte, Germany) using a Lipex extrusion device (Avestin Inc., Toronto, Canada). Unentrapped ammonium sulfate was removed by centrifugation. Small unilamellar colloidal vesicles were suspended in an isotonic solution (2 ml) of GEM and kept at room temperature for 3 hours. The unentrapped drug was removed by centrifugation, yielding PEGylated liposomes encapsulating GEM (PEG-lipo-GEM).

Conjugation of antibody to liposomes

PDP-PEG-lipo-GEM was thiolated by treatment with 25 mM DTT in PBS (pH 7.0) for 30 minutes at room temperature. SH-PEG-lipo-GEM was separated from unbound DTT by gel chromatography using a Sephadex G-50 column. The CD133-Ab for conjugation, dissolved in PBS, was reacted with succinimidyl 4-(*p*-maleimidophenyl)butyrate (SMPB) crosslinker, prepared freshly at 25 mM in dimethylformamide, at room temperature to give a 20 : 1 molar ratio of SMPB : CD133-Ab. After a 30 minute reaction, the MPB-CD133-Ab was separated from the reactants by gel chromatography on a Sephadex G-75 column. SH-PEG-lipo-GEM was incubated with MPB-CD133-Ab at a 250 : 1 (wt/wt) ratio overnight at room temperature.

Physicochemical characterization of liposomes

The encapsulation efficiency of GEM into liposomes was evaluated using the Bligh and Dyer extraction method.[37] Briefly, 100 μl of liposomes was mixed with 150 μl of PBS, 250 μl of methanol, and 1 ml of chloroform in a glass tube to form a homogeneous solution. After centrifugation, the mixture was separated into two distinct layers: a lower organic layer containing phospholipids and other hydrophobic materials, and an upper aqueous layer containing GEM and other hydrophilic materials. The organic phase was removed, chloroform was

added again, and the mixture was centrifuged. These procedures were repeated three times. The amount of GEM in the supernatant was determined spectrophotometrically at 268 nm using an UltraSpec 2000 UV-vis spectrophotometer (Pharmacia Biotech, Cambridge, UK). The size distributions and zeta potentials of the liposomes were determined with a dynamic laser-light scattering system (NICOMP 380ZLS; Particle Sizing Systems Inc., Santa Barbara, CA, USA) using a He–Ne laser light source. Measurements were carried out at room temperature with a 90 degree detection angle.

Serum protein adsorption assay

The adsorption of serum proteins onto liposomes was estimated by measuring the amount of bovine serum albumen (BSA) bound to liposomes *in vitro*. Non-PEGylated liposomes without the drug (non-PEG-lipo-empty), PEG-lipo-empty, PEG-lipo-GEM and PEG-lipo-CD133-GEM were incubated with 1% (w/v) BSA dissolved in PBS (pH 7.4) at 37 °C. After incubation for 0.5, 3, 12, 24 and 48 hours, samples were centrifuged at 13 000 × *g* for 15 minutes. The free BSA in the supernatant was removed, and the liposomes were washed three times with PBS followed by centrifugation at 13 000 × *g* for 15 minutes. The amount of proteins adsorbed onto the liposomes was measured with a BCA Protein Assay Kit (Pierce, Rockford, IL, USA) using BSA as a standard. Samples (25 μl) were added into 96 well plates and mixed with 200 μl of BCA working reagent. The absorbance was measured spectrophotometrically at 570 nm using a 1420 Multilabel Counter (Victor3; PerkinElmer Life and Analytical Sciences, Waltham, MA, USA).

Apoptosis assay

The effects of various formulations on cell apoptosis were assessed by the Annexin V-FITC/PI staining kit (Becton Dickenson, San Diego, CA, USA). GSCs (5×10^5) were seeded onto 6 mm plates and treated with PBS (control), PEGylated liposomes without drug (PEG-lipo-empty), free GEM, PEG-lipo-GEM and PEG-lipo-CD133-GEM for 24 hours at 37 °C. Each formulation except PBS and PEG-lipo-empty contained an equivalent amount of GEM (0.47 μM). The cells were then washed three times and stained with Annexin V-FITC and PI according to the instructions of the manufacturer. Cell samples were observed by fluorescence microscopy (IX71IX51; Olympus, Tokyo, Japan) and apoptotic fractions were determined by flow cytometry using FACSCalibur (Becton Dickenson, San Jose, CA, USA). To compensate for the spillover between the FITC and PI fluorescence signals, we adjusted the flow cytometer settings using unstained, FITC-only, and PI-only controls.

In vitro anti-proliferation assay

GSCs (2×10^4), seeded into 48-well tissue culture plates and incubated for 24 hours at 37 °C, were dissociated and treated with PBS, PEG-lipo-empty, free GEM, PEG-lipo-GEM or PEG-lipo-CD133-GEM for 48 hours. After incubation, cell growth was determined by MTT assay, as described above.

Pharmacokinetic and biodistribution studies

For the pharmacokinetic and biodistribution study, fluorescently (Cy5.5) labeled GEM, prepared by chemical modification of GEM, was used. Liposome formulations with GEM were prepared, and their encapsulating efficiency was measured using a fluorescence plate reader at $\lambda_{ex} = 685$ nm and $\lambda_{em} = 705$ nm. Male, 4-week-old, ICR mice (Jung-Ang Lab Inc., Seoul, Korea) (18–20 g) were injected intravenously (i.v.) with GEM in various formulations at a dose of 0.951 mg kg^{-1}. Blood samples (40 μl) were collected retro-orbitally at 1, 2, 5, 10, 20, 30, 60, 120, 240 and 480 minutes after injection, and serum was isolated. A 15 μl aliquot of serum was mixed with 35 μl of 10% Triton X-100 in PBS and incubated at 65 °C for 10 minutes, after which 200 μl methanol was added and the samples were incubated at 65 °C for an additional 10 minutes. The samples were centrifuged in a microfuge at 14 000 rpm for 5 minutes, and 200 μl of the supernatant was transferred to a black 96-well plate (SPL Life Science, Pocheon, Korea). The fluorescence intensity of the sample was measured using a plate reader at $\lambda_{ex} = 685$ nm and $\lambda_{em} = 705$ nm. The concentration of GEM in each sample was calculated from a standard curve. For determination of biodistribution by *in vivo* imaging, BALB/c nude mice were inoculated subcutaneously on the right back with 1×10^6 GSCs. Once the tumors had reached about 400–500 mm^3, the tumor-bearing mice were injected *via* the tail vein with GEM in different formulations at a dose of 0.0317 mg kg^{-1}. At different points of time, after the injection, the mice were subjected to inhalation anesthesia, and *in vivo* images were acquired and recorded using an *in vivo* imaging system (IVIS; Xenogen Co., Alameda, CA, USA) with a built-in CCD camera. The images and the fluorescence signals were analyzed using Xenogen Living Image Software (Xenogen Co.). After 96 hours, the mice were killed, and the major organs, including the liver, kidney, lung and heart, and the tumor were dissected and imaged.

Anti-tumor assay in nude mice

Male immunodeficient mice were maintained on a 12 hour light/dark cycle in appropriately isolated cages with free access to drinking water and food. U87 GSC cells were collected and resuspended in PBS. A total of 1.0×10^6 cells in 70 μl of PBS was inoculated subcutaneously into the right flank of each nude mouse. Two weeks after cell injection, when tumor volumes had reached about 50 mm^3 (day 0), mice were randomly divided into five groups ($n = 6$ mice per group): (a) PBS (control), (b) PEG-lipo-empty, (c) free GEM, (d) PEG-lipo-GEM (50 mg kg^{-1}) and (e) PEG-lipo-CD133-GEM (50 mg kg^{-1}). Each formulation was intravenously injected into mice twice a week for 4 weeks for a total of eight injections.

Statistical analysis

Data are presented as mean ± standard deviation (SD). *In vivo* parameters are expressed as mean ± standard error (SE). Statistical analyses were performed using Student's *t*-test. Statistical significance was assigned for *P*-values < 0.05 (95% confidence level) or < 0.01 (99% confidence level).

Results

Isolation and characterization of GSCs

It has been reported that CD133 expression is a typical feature of GSCs.[10] GSCs can be cultured in suspension in serum-free medium supplemented with B27, bFGF and hEGF, generating floating spheroid bodies.[4] The GSC population in U87 cells was evaluated by dissociating floating spheroid bodies and sorting them using the magnetic-activated cell sorting (MACS) method employing CD133-Ab magnetic beads. As shown in Fig. 1A, CD133-Ab-sorted cells (GSCs) indeed formed spheroid bodies, exhibiting a significantly higher ability to form spheroid bodies than $CD133^-$ or unsorted U87 cells. CD133 expression in the different cell populations was directly analyzed by Western blotting and quantified by FACS. As shown in Fig. 1B and C, CD133 expression levels were significantly higher in CD133-Ab-sorted GSCs than in $CD133^-$ or unsorted U87 cells. The percentages of CD133 expression cells determined by FACS analysis were 5.4% in unsorted U87 cells, 0% in $CD133^-$ cells and 90.5% in GSCs. Another defining feature of GSCs is their more rapid proliferation. As shown in Fig. 1D, the cell growth rate of GSCs cultured in DMEM containing 10% FBS as determined by the MTT assay was higher compared to that of the unsorted U87 cells ($P < 0.05$). The property of resistance to chemotherapy is a major clinical criterion characteristic of cancer stem cells.[11,38–42] To measure chemoresistance, we determined the IC_{50} value for cell growth inhibition by GEM using MTT assays. The IC_{50} values for GEM were about 50-times higher in GSCs than in the unsorted U87 cells (Fig. 1E). Thus, GSCs were significantly resistant to the chemotherapeutic drug, GEM, compared with unsorted U87 cells. Thus, compared to unsorted U87 cells, GSCs exhibited greater chemoresistance

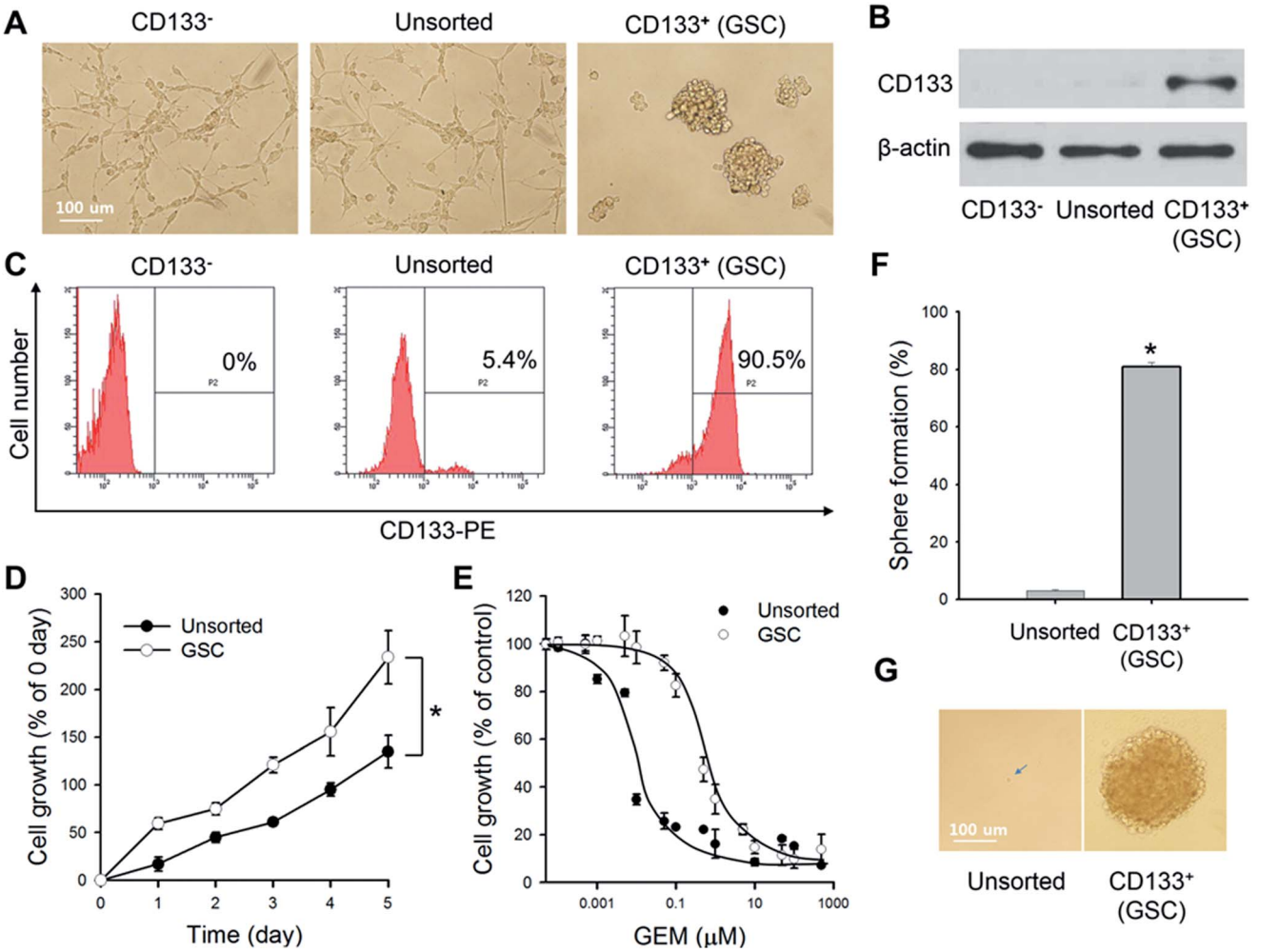

Fig. 1 Characterization of GSCs. (A) Changes in U87 cell morphology after sorting cells were examined by bright-field microscopy (scale bar = 100 μm). Western blot (B) and FACS (C) analyses were performed using anti-CD133 antibodies. CD133 expression in subpopulations of U87 cells was determined by calculating the percentages of CD133-PE-conjugated cells by FACS. (D) Growth rates of GSCs and unsorted U87 cells cultured in DMEM containing 10% FBS were determined by MTT assay. (E) Effect of GEM on the growth characteristics of GSCs and unsorted U87 cells *in vitro* was analyzed. Each cell population was treated with different concentrations of anti-cancer drugs for 48 hours, and growth rates were determined by MTT assay. (F) Percentages of secondary spheres formed in wells seeded with individual GSCs and unsorted U87 cells were determined. (G) Representative photographs of secondary spheres were determined by bright microscopy (scale bar = 100 μm). Data shown represent the mean ± SD of three experiments (*$P < 0.05$).

and a higher proliferation rate. Collectively, these results demonstrate the successful separation and verification of GSCs from the U87 GBM cell line.

Tumor spheres formation assay

A single-cell suspension prepared from tumor GSCs and unsorted U87 cell line was examined for the capacity to form secondary spheres by single parental cells in fresh serum-free DMEM/F12 medium. Fig. 1F and G show that secondary spheres were formed in the wells seeded with cells from tumor spheres at a rate of 81.0 ± 3.21%. The unsorted U87 cells showed a rate of sphere formation at 1.57 ± 0.34%.

Tumorigenic capacity of GSCs in BALB/c nude mice

The tumorigenic capacities of unsorted U87 cells and GSCs were measured *in vivo*. To generate xenografts, we injected the right flank of nude mice with GSCs or unsorted U87 cells (1×10^6 cells in 70 μl PBS). Mice were observed twice a week and sacrificed at 42 days. Both unsorted U87 cells and GSCs were capable of initiating gliomas in 20 days; however, mice inoculated with the latter cell type exhibited enhanced tumor growth. As shown in Fig. 2, after 42 days, the mean tumor volume in the GSC-injected group was about 10 times larger than that in groups injected with unsorted U87 cells ($P < 0.05$).

Physicochemical characterization of liposomes

The characteristics of liposomes containing GEM used in this study are summarized in Table 1. The average diameter of non-PEG-lipo-empty, PEG-lipo-empty, PEG-lipo-GEM and PEG-lipo-CD133-GEM was approximately 132 ± 45.3, 145 ± 66.6, 128 ± 71.4 and 156 ± 56.1 nm, respectively. All of the liposomes tested maintained a negative charge of approximately −10 mV. The GEM encapsulation efficiency of the different formulations was found to be about 50–70%. The amounts of CD133-Ab attached to the liposomes were determined by the Bradford assay,[43] and the concentration of phospholipids was measured by phosphorus assay after lipid extraction.[37,44] Based on these measurements and the assumptions that the thickness of the lipid bilayer of the liposomes was 40 Å and the area occupied by each phospholipid was 70–75 $Å^2$, the number of CD133-Ab attached to one liposome was 15.[45,46]

Table 1 Characterization of GEM-containing liposomes

Sample	Particle size (nm)	Zeta potential (mV)	Encapsulation efficiency (%)
Non-PEG-lipo-empty	132 ± 45	−8.21 ± 3.13	—
PEG-lipo-empty	145 ± 67	−12.31 ± 4.69	—
PEG-lipo-GEM	128 ± 71	−7.40 ± 2.82	71.3 ± 10.3
PEG-lipo-CD133-GEM	156 ± 56	−9.70 ± 3.70	54.2 ± 17.5

Serum protein adsorption of PEGylated liposomes *in vitro*

Adsorption of serum protein onto liposomes has the potential to cause aggregation and instability of liposomes in the blood. Thus, the amount of protein adsorbed onto the surface of liposomes was measured by BCA protein assay. As shown in Fig. 3, the amount of protein adsorbed onto non-PEG-lipo-empty liposomes increased over the course of a 48 hour incubation period, whereas PEGylated liposomes, with or without GEM, showed only a small amount of protein adsorption. Specifically, PEGylated liposomes (PEG-lipo-empty, PEG-lipo-GEM and PEG-lipo-CD133-GEM) adsorbed about 2.5-fold less protein than non-PEG-lipo-empty liposomes in 48 hours ($P < 0.01$). The absence of significant protein adsorption or aggregation of PEGylated liposomes presumably reflects the fact that PEG coats the surface of liposomes, creating a steric barrier to water that results in repulsive interactions between PEG and serum proteins.

Apoptosis assay

To confirm that our formulation is capable of producing a greater degree of apoptosis than the free drug, we examined apoptosis by Annexin V FITC/PI staining 24 hours after

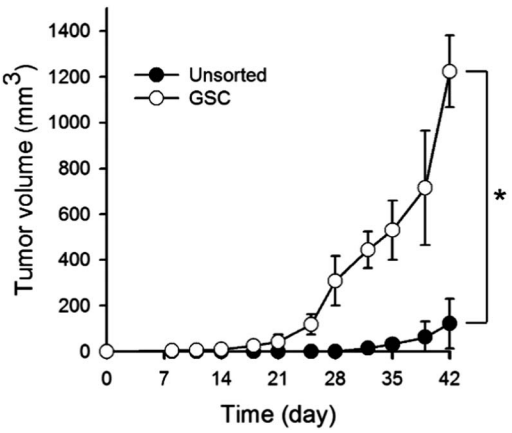

Fig. 2 Subcutaneous tumorigenicity in nude mice. Tumor growth rate in mice with severe combined immunodeficiency was measured after subcutaneous inoculation of 1×10^6 GSCs or unsorted U87 cells. Data shown represent the mean ± SE of four experiments (*$P < 0.05$).

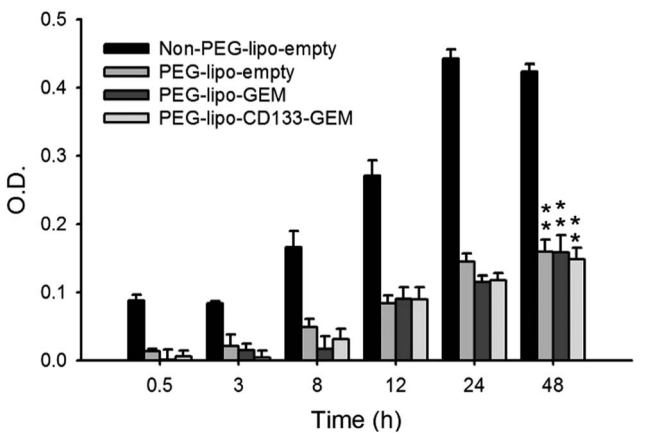

Fig. 3 Protein adsorption onto liposomes in a 1% BSA solution. Data shown represent the mean ± SD of four experiments (**$P < 0.01$).

treatment. Fluorescent apoptotic bodies were observed by fluorescence microscopy (Fig. 4A) and quantified by FACS (Fig. 4B). There was a marked increase in apoptotic bodies in cells treated with PEG-lipo-CD133-GEM liposomes compared to cells treated with PBS or other formulations. These results clearly demonstrate that our designed formulation, PEG-lipo-CD133-GEM, exerts greater cytotoxicity toward GSCs.

Inhibition of proliferation of GSCs

To investigate the anti-proliferative effects of GEM in various formulations toward GSCs, we treated GSCs with PBS (control), PEG-lipo-empty, free GEM, PEG-lipo-GEM or PEG-lipo-CD133-GEM for 48 hours. As shown in Fig. 5, the anti-proliferative effect of PEG-lipo-GEM was greater than that of the free drug; this effect was further enhanced in liposomes conjugated with CD133. Specifically, the anti-proliferative effect of PEG-lipo-CD133-GEM was more than 2 times higher than that of free GEM ($P < 0.01$), presumably reflecting the specific targeting of the CD133 surface marker by PEG-lipo-CD133-GEM and the enhanced stability and uptake of the PEGylated liposome formulation. Neither PBS control nor PEG-lipo-empty affected the proliferation of GSCs.

Pharmacokinetic studies

Plasma concentration–time profiles were calculated after i.v. injection of various formulations of GEM into ICR mice (Fig. 6), and pharmacokinetic parameters were calculated using a two-compartment model (Table 2). Free GEM rapidly disappeared from the blood and was not detected after 240 minutes. With PEGylated liposomes, the half-life ($t_{1/2\alpha}$ and $t_{1/2\beta}$) and area under the curve (AUC) increased and the total clearance (CL_t) decreased. Compared to free GEM, the AUC of PEG-lipo and PEG-lipo-CD133 increased by 6.95 and 7.28 times, respectively (21 *vs.* 146 and 153 μg min ml^{-1}). The CL_t of PEG-lipo-GEM and PEG-lipo-CD133-GEM formulations both decreased by 6.67 times compared with that of free GEM, suggesting that the PEGylated liposome increased the stability of GEM in the blood and thus prolonged its half-life. The mean residence time MRT of PEG-lipo-GEM (468 minutes) and PEG-lipo-CD133-GEM (374 minutes) formulations also increased about 8.35 and 6.67 times, respectively, compared to that of the free GEM (56 minutes). These results clearly show that overall pharmacokinetic behaviors are improved using PEGylated liposomes as a delivery system for GEM.

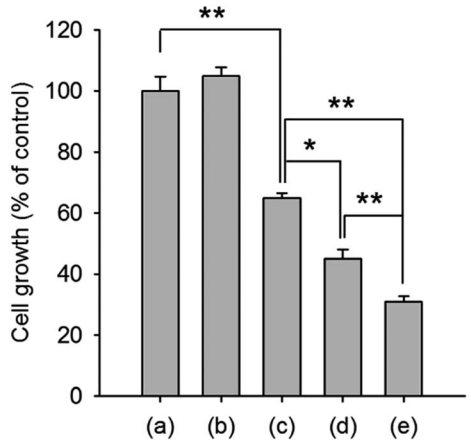

Fig. 5 *In vitro* growth-inhibitory activity of various GEM formulations towards GSCs. GSC growth was measured by MTT assay after treatment with (a) PBS, (b) PEG-lipo-empty, (c) free GEM, (d) PEG-lipo-GEM or (e) PEG-lipo-CD133-GEM. Data shown represent the mean ± SD of four experiments (*$P < 0.05$, **$P < 0.01$).

Biodistribution

To investigate the *in vivo* biodistribution of GEM in PEGylated liposomes, we injected the fluorescently labeled GEM in various

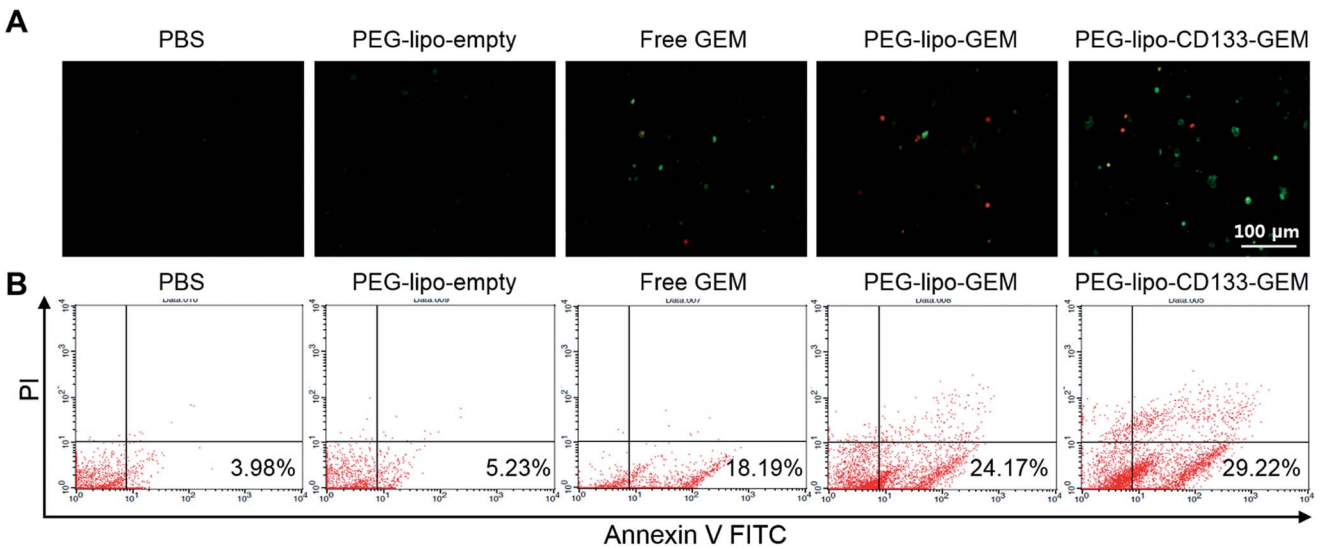

Fig. 4 Analysis of apoptosis in GSCs was carried out using Annexin V–FITC and PI after treatment with GEM in various formulations. Cells were treated with each formulation for 24 hours, then stained with Annexin V–FITC and PI for 15 minutes. (A) Morphology of apoptotic GSCs was observed by fluorescence microscopy (scale bar = 100 μm). (B) Percentages of apoptotic GSCs were quantified by FACS.

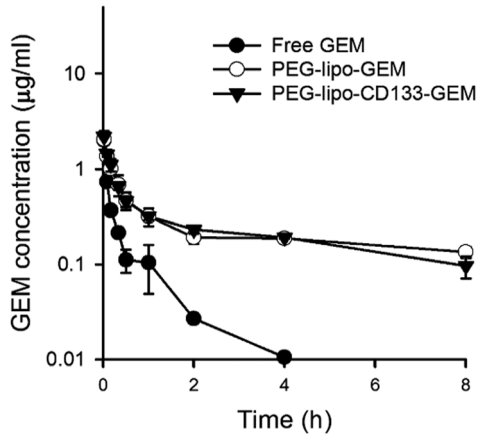

Fig. 6 Plasma concentration–time profiles of GEM in various formulations. For measuring the concentration of GEM in plasma, fluorescently (Cy5.5) labeled GEM, prepared by chemical modification of GEM, was used. The plasma concentration of GEM after i.v. injection of free GEM, PEG-lipo-GEM or PEG-lipo-CD133-GEM in mice was determined using a fluorescence microplate reader. Data shown represent the mean ± SE of three experiments.

formulations into nude mice bearing GSC tumor xenografts and monitored GEM fluorescence *in vivo* at different time points using an IVIS imaging system. Fluorescence was not observed 48 hours after tail vein injection, except in mice injected with PEG-lipo-GEM or PEG-lipo-CD133-GEM (Fig. 7A). Fluorescence signals in mice injected with PEG-lipo-GEM and PEG-lipo-CD133-GEM were detected 96 hours after injection which is about 14 times the half-life of the free GEM in blood. This phenomenon is presumably due to the accumulation of GEM in tissues. As the IVIS system could detect the fluorescence signals of GEM both in plasma and tissues, the apparent fluorescence signals in mice injected with GEM in PEGylated liposomes were detected for such a long time. To more precisely compare the fluorescence signals, we dissected the tumor and the major organs 96 hours after injection. This *ex vivo* analysis showed

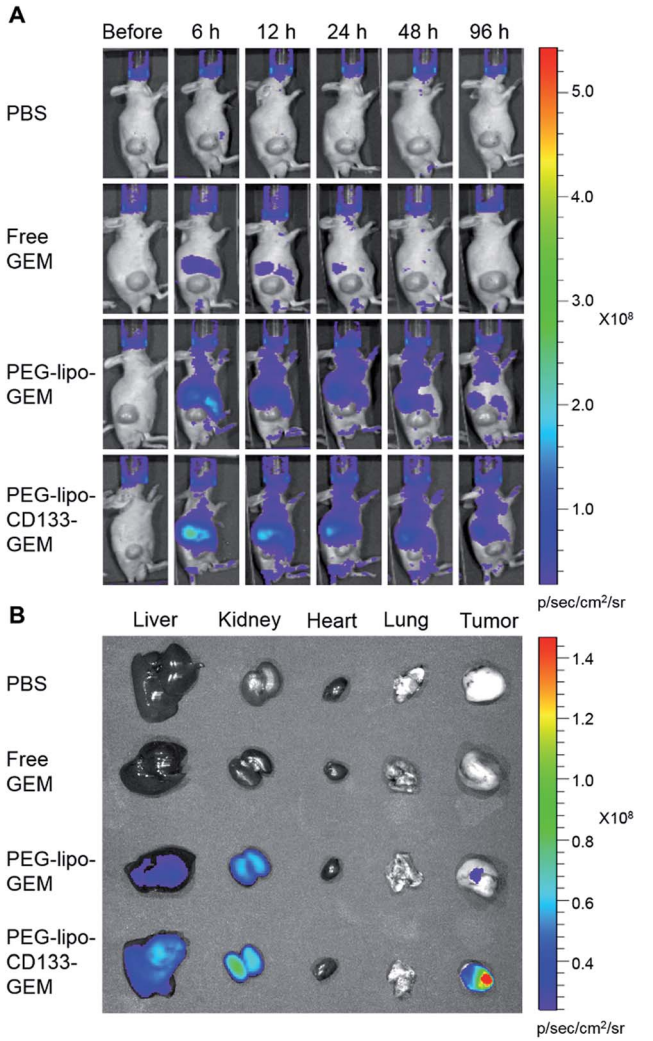

Fig. 7 Biodistribution of GEM in various formulations. For detecting biodistribution of GEM in mice, fluorescently (Cy5.5) labeled GEM was used. Whole-body images (A) and *ex vivo* images of dissected organs (B) after i.v. injection of tumor-bearing BALB/c nude mice with GEM in various formulations were obtained by IVIS.

Table 2 Pharmacokinetic parameters of GEM after i.v. administration (0.951 mg kg^{-1}) in various formulations

		Formulation		
Parameter		Free GEM	PEG-lipo-GEM	PEG-lipo-CD133-GEM
A	($\mu g\ ml^{-1}$)	2.39 ± 0.19	1.91 ± 0.30	2.02 ± 0.11
B	($\mu g\ ml^{-1}$)	0.065 ± 0.001	0.245 ± 0.041	0.358 ± 0.076
α	(min^{-1})	0.196 ± 0.002	0.106 ± 0.025	0.100 ± 0.019
β	(min^{-1})	0.00748 ± 0.00030	0.00194 ± 0.00022	0.00318 ± 0.00096
k_{12}	(min^{-1})	0.0728 ± 0.0006	0.0805 ± 0.0232	0.0708 ± 0.0191
k_{21}	(min^{-1})	0.0122 ± 0.0001	0.0134 ± 0.0020	0.0158 ± 0.0009
k_{10}	(min^{-1})	0.124 ± 0.000	0.015 ± 0.001	0.017 ± 0.002
$t_{1/2\alpha}$	(min)	3.48 ± 0.03	7.47 ± 1.58	8.05 ± 1.83
$t_{1/2\beta}$	(min)	92 ± 0	372 ± 47	296 ± 83
AUC	($\mu g\ min\ ml^{-1}$)	21 ± 0	146 ± 13	153 ± 23
MRT	(min)	56 ± 1	468 ± 75	374 ± 118
Vd_{ss}	($ml\ kg^{-1}$)	2480 ± 199	3205 ± 758	2216 ± 472
AUMC	($\mu g\ min^2\ ml^{-1}$)	1221 ± 14	66342 ± 6260	64918 ± 28994
CL_t	($ml\ min^{-1}$)	44.0 ± 0.2	6.6 ± 0.5	6.7 ± 0.9

that PEG-lipo-GEM and PEG-lipo-CD133-GEM accumulated in the tumor (Fig. 7B). Notably, PEG-lipo-CD133-GEM showed greater accumulation in the tumor than did PEG-lipo-GEM.

Anti-tumor study in xenograft models

The anti-tumor activity of various formulations of GEM was measured in BALB/c nude mice bearing GSC tumor xenografts by analyzing the tumor volume after i.v. injection of PBS, PEG-lipo-empty, free GEM, PEG-lipo-GEM or PEG-lipo-CD133-GEM ($n = 6$ mice per group). Drug administration started on day 3 and was repeated on days 7, 10, 14, 17, 21, 24 and 28. Tumor volume was measured twice a week until day 32. Tumor volumes in mice treated with the various formulations changed differently after injection. As shown in Fig. 8A, tumors in the PBS- or empty-lipo-treated group reached an average volume about 30 times larger than that at day 0, whereas tumor volumes in the PEG-lipo-CD133-GEM-treated group were only about 2 times larger, which is a 15-fold difference in tumor volume. The volume of tumors in the group treated with PEG-lipo-CD133-GEM was less than that in the PEG-lipo-GEM-treated group, which, in turn, was less than that of the free-GEM-treated group. However, treatment with free-GEM (50 mg kg^{-1}) was associated with severe toxicity, as evidenced by a marked (~20%) weight loss in the animals in this group (Fig. 8B). In contrast, neither PEG-lipo-GEM nor PEG-lipo-CD133-GEM treatment caused severe reduction in body weight, suggesting much lower toxicity of these liposome formulations.

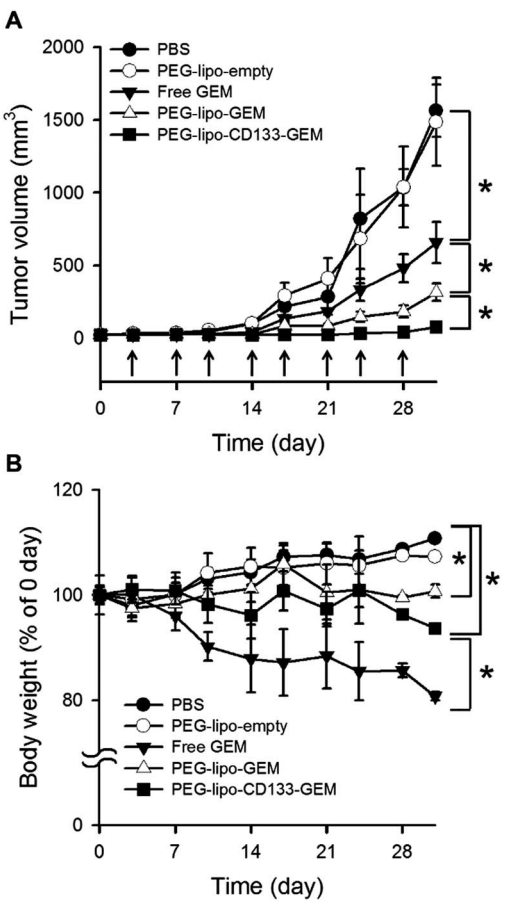

Fig. 8 Tumor growth inhibition (A) and changes in mean body weight (% of day 0) (B) produced in nude mice bearing GSC tumor xenografts by i.v. treatment with various GEM formulations. Tumor-bearing mice were administered various formulation of GEM (i.v.) twice a week on days 3, 7, 10, 14, 17, 21, 24 and 28 for a total of eight doses (indicated by arrows in the figure). Data shown represent the mean ± SE of seven experiments (*$P < 0.05$).

Discussion

GBM remains a highly lethal and recurrent disease. Even if treated surgically, the prognosis of GBM patients is poor, with a 5 year survival rate of only 5%.[47] GSCs have been regarded as the basis for the failure of current therapeutic options. GEM is among the effective agents against GBM *in vivo*, but its use in targeting GSCs is limited owing to its insufficient therapeutic efficacy. To overcome these limitations and enhance the anti-GSC effect of GEM, we designed new GEM-encapsulating liposome formulations. Although the concepts of PEGylation and antibody-targeting have previously been explored individually by various researchers, in this study, we have combined these concepts in GEM-encapsulating liposomes for the treatment of GSCs. By combining these properties, it was possible to achieve the benefits of both properties, resulting in an increased or synergistic therapeutic efficacy.

For targeting studies, we separated GSCs from the U87 GBM cells using an anti-CD133 antibody-based strategy and confirmed their properties (Fig. 1 and 2). The physicochemical properties of various liposomes containing GEM were also elucidated using particle size analyses and zeta potential measurements. Matsumura *et al.* have reported the enhanced permeability and retention (EPR) effect, the property by which molecules of certain sizes, typically liposomes, nanoparticles and macromolecular drugs, tend to accumulate in tumor tissue to a much greater degree than in normal tissues.[48] Liposome with a diameter greater than 400 nm has a very limited circulation in the blood stream because it is quickly captured by the RES, whereas liposome with a diameter smaller than 200 nm can remain in the circulation for a long time.[49,50] The charge on the surface of a liposome influences its biodistribution, stability, kinetics and interactions with targeted cells. Negatively charged liposomes are less prone to aggregation and are comparatively more stable in suspension.[51] Therefore, we prepared liposomes for GSC targeting of the appropriate particle size (100–200 nm) and zeta potential (0 to −20 mV) (Table 1). We also confirmed that the amount of protein adsorption onto GEM-encapsulating PEGylated liposomes was significantly decreased compared to that of non-PEGylated liposomes (Fig. 3) owing to the steric barrier to water created by the surface coating of PEG, which results in repulsive interactions between the PEG chain and serum proteins. These findings established the usefulness of PEGylated liposomes as a suitable drug carrier for targeting GSCs *in vivo*.

CD133-Ab, used as a targeting ligand, significantly enhanced the delivery of GEM-loaded PEGylated liposomes through the endocytosis of CD133, resulting in the apoptosis of the cells (Fig. 4). This result is consistent with the results of MTT assays,

which collectively showed that PEG-lipo-CD133-GEM exerted an enhanced cytotoxicity toward GSCs through the induction of apoptosis (Fig. 5). On the basis of these results, we used the PEG-lipo-CD133-GEM formulation for *in vivo* pharmacokinetic, biodistribution and anti-tumor efficacy studies.

To determine the effect of PEGylation on the pharmacokinetics of PEGylated liposomes, we compared the pharmacokinetics of PEG-lipo-GEM and PEG-lipo-CD133-GEM to that of free GEM. Free GEM was rapidly eliminated from the blood stream, whereas PEG-lipo-GEM and PEG-lipo-CD133-GEM exhibited extended circulation times as a result of PEGylation (Fig. 6). The AUC and half-life of GEM were also increased in PEGylated liposome formulations, and its clearance rate was decreased (Table 2). Thus, PEGylation seems to successfully protect nanoparticles from RES uptake.

To test whether this prolongation of circulation time increased the accumulation of GEM in tumors *via* the EPR effect, we performed *in vivo* imaging of tissues in tumor-bearing nude mice injected i.v. with GEM in various formulations. GEM fluorescence was observed *in vivo* up to 96 hours after injection of GEM in PEGylated liposomes, whereas fluorescence intensity diminished rapidly after injection of free GEM (Fig. 7A). In an *ex vivo* study, GEM fluorescence signals were stronger in tumors from mice injected with PEG-lipo-CD133-GEM than in those from mice injected with PEG-lipo-GEM (Fig. 7B). Results of both *in vivo* and *ex vivo* studies suggest that the increased targeting ability of GEM afforded by CD133-Ab conjugation enabled GEM to effectively accumulate in GSC tumor xenografts.

PEG-lipo-CD133-GEM exerted significant anti-tumor efficacy, promoting greater regression of established GSC tumors in the nude mouse xenograft model. The tumor volumes in these groups were much smaller than those in other groups (Fig. 8A). The delivery of GEM to the tumor cells was enhanced presumably through binding of CD133-Abs to the CD133 surface markers in GSCs. Liposomes containing PEG chains terminally modified by conjugation of CD133-Abs appeared to be highly stable with long circulation times *in vivo*. Thus, the Ab-liposome drug delivery system containing GEM described here effectively suppressed tumor growth by virtue of the targeting capability of the CD133-Ab of the liposome. Moreover, monitoring of body weight changes showed that PEGylation significantly reduced the toxicity of GEM in liposomes compared with free GEM in xenograft models (Fig. 8B). These findings clearly suggest that PEG-lipo-CD133-GEM exhibits comparable efficacy in inhibiting tumor growth, but is much less toxic compared to the same dose of free GEM.

Conclusions

We have designed a CD133-conjugated PEGylated liposome encapsulating GEM for the targeting of glioblastoma stem cells and this system clearly showed an enhanced delivery of GEM to the GSCs, resulting in the inhibition of the cells both *in vitro* and in xenograft models. With further investigation, this delivery system could serve as an effective and safe molecular therapeutics for the treatment of GBM.

Acknowledgements

This work was supported by the National Research Foundation of Korea (NRF) grant funded by the Korea government (MSIP) (no. 2011-0030074).

Notes and references

1 H. Ohgaki and P. Kleihues, *J. Neuropathol. Exp. Neurol.*, 2005, **64**, 479–489.
2 P. Y. Wen and S. Kesari, *N. Engl. J. Med.*, 2008, **359**, 492–507.
3 R. R. Malla, S. Gopinath, K. Alapati, B. Gorantla, C. S. Gondi and J. S. Rao, *Neuro-Oncology*, 2012, **14**, 745–760.
4 S. Bao, Q. Wu, R. E. McLendon, Y. Hao, Q. Shi, A. B. Hjelmeland, M. W. Dewhirst, D. D. Bigner and J. N. Rich, *Nature*, 2006, **444**, 756–760.
5 D. M. Park and J. N. Rich, *Mol. Cells*, 2009, **28**, 7–12.
6 S. K. Singh, I. D. Clarke, M. Terasaki, V. E. Bonn, C. Hawkins, J. Squire and P. B. Dirks, *Cancer Res.*, 2003, **63**, 5821–5828.
7 M. Al-Hajj, M. S. Wicha, A. Benito-Hernandez, S. J. Morrison and M. F. Clarke, *Proc. Natl. Acad. Sci. U. S. A.*, 2003, **100**, 3983–3988.
8 C. A. O'Brien, A. Pollett, S. Gallinger and J. E. Dick, *Nature*, 2007, **445**, 106–110.
9 S. Miraglia, W. Godfrey, A. H. Yin, K. Atkins, R. Warnke, J. T. Holden, R. A. Bray, E. K. Waller and D. W. Buck, *Blood*, 1997, **90**, 5013–5021.
10 S. K. Singh, C. Hawkins, I. D. Clarke, J. A. Squire, J. Bayani, T. Hide, R. M. Henkelman, M. D. Cusimano and P. B. Dirks, *Nature*, 2004, **432**, 396–401.
11 S. K. Singh, I. D. Clarke, M. Terasaki, V. E. Bonn, C. Hawkins, J. Squire and P. B. Dirks, *Cancer Res.*, 2003, **63**, 5821–5828.
12 F. Zeppernick, R. Ahmadi, B. Campos, C. Dictus, B. M. Helmke, N. Becker, P. Lichter, A. Unterberg, B. Radlwimmer and C. C. Herold-Mende, *Clin. Cancer Res.*, 2008, **14**, 123–129.
13 D. Beier, J. Wischhusen, W. Dietmaier, P. Hau, M. Proescholdt, A. Brawanski, U. Bogdahn and C. P. Beier, *Brain Pathol.*, 2008, **18**, 370–377.
14 S. K. Swaminathan, E. Roger, U. Toti, L. Niu, J. R. Ohlfest and J. Panyam, *J. Controlled Release*, 2013, **171**, 280–287.
15 C. H. Wang, S. H. Chiou, C. P. Chou, Y. C. Chen, Y. J. Huang and C. A. Peng, *Nanomedicine*, 2011, **7**, 69–79.
16 E. Mini, S. Nobili, B. Caciagli, I. Landini and T. Mazzei, *Ann. Oncol.*, 2006, **17**(suppl. 5), v7–v12.
17 P. K. Julka, T. Puri and G. K. Rath, *Hepatobiliary Pancreatic Dis. Int.*, 2006, **5**, 110–114.
18 A. Duenas-Gonzalez, J. J. Zarba, F. Patel, J. C. Alcedo, S. Beslija, L. Casanova, P. Pattaranutaporn, S. Hameed, J. M. Blair, H. Barraclough and M. Orlando, *J. Clin. Oncol.*, 2011, **29**, 1678–1685.
19 S. Madajewicz, D. M. Waterhouse, P. S. Ritch, M. Q. Khan, D. J. Higby, C. G. Leichman, S. K. Malik, P. Hentschel, J. F. Gill, L. Zhao and S. J. Nicol, *Invest. New Drugs*, 2012, **30**, 772–778.
20 J. D. Pitts, *Mol. Carcinog.*, 1994, **11**, 127–130.

21 S. Cottin, K. Ghani, P. O. de Campos-Lima and M. Caruso, *Mol. Cancer*, 2010, **9**, 141.
22 F. Fehlauer, M. Muench, E. J. Smid, B. Slotman, E. Richter, P. Van der Valk and P. Sminia, *Oncol. Rep.*, 2006, **15**, 97–105.
23 A. Fabi, A. Mirri, A. Felici, A. Vidiri, A. Pace, E. Occhipinti, F. Cognetti, G. Arcangeli, B. Iandolo, M. A. Carosi, G. Metro and C. M. Carapella, *J. Neuro. Oncol.*, 2008, **87**, 79–84.
24 W. Wick, M. Hermisson, R. D. Kortmann, W. M. Kuker, F. Duffner, J. Dichgans, M. Bamberg and M. Weller, *J. Neuro. Oncol.*, 2002, **59**, 151–155.
25 A. I. Minchinton and I. F. Tannock, *Nat. Rev. Cancer*, 2006, **6**, 583–592.
26 L. A. Huxham, A. H. Kyle, J. H. Baker, L. K. Nykilchuk and A. I. Minchinton, *Cancer Res.*, 2004, **64**, 6537–6541.
27 M. Choi, D. H. Shin and J. Kim, *J. Pharm. Invest.*, 2013, **43**, 461–469.
28 V. P. Torchilin, *Nat. Rev. Drug Discovery*, 2005, **4**, 145–160.
29 D. Papahadjopoulos, T. M. Allen, A. Gabizon, E. Mayhew, K. Matthay, S. K. Huang, K. D. Lee, M. C. Woodle, D. D. Lasic, C. Redemann, *et al.*, *Proc. Natl. Acad. Sci. U. S. A.*, 1991, **88**, 11460–11464.
30 Y. H. Bae and K. Park, *J. Controlled Release*, 2011, **153**, 198–205.
31 S. D. Li and L. Huang, *J. Controlled Release*, 2010, **145**, 178–181.
32 C. Celia, N. Malara, R. Terracciano, D. Cosco, D. Paolino, M. Fresta and R. Savino, *Nanomedicine*, 2008, **4**, 155–166.
33 D. Cosco, A. Bulotta, M. Ventura, C. Celia, T. Calimeri, G. Perri, D. Paolino, N. Costa, P. Neri, P. Tagliaferri, P. Tassone and M. Fresta, *Cancer Chemother. Pharmacol.*, 2009, **64**, 1009–1020.
34 C. Celia, M. G. Calvagno, D. Paolino, S. Bulotta, C. A. Ventura, D. Russo and M. Fresta, *J. Nanosci. Nanotechnol.*, 2008, **8**, 2102–2113.
35 S. C. Yu, Y. F. Ping, L. Yi, Z. H. Zhou, J. H. Chen, X. H. Yao, L. Gao, J. M. Wang and X. W. Bian, *Cancer Lett.*, 2008, **265**, 124–134.
36 R. K. Kim, M. J. Kim, C. H. Yoon, E. J. Lim, K. C. Yoo, G. H. Lee, Y. H. Kim, H. Kim, Y. B. Jin, Y. J. Lee, C. G. Cho, Y. S. Oh, M. C. Gye, Y. Suh and S. J. Lee, *Mol. Pharmacol.*, 2012, **82**, 400–407.
37 B. Eg and D. Wj, *Can. J. Biochem. Physiol.*, 1959, **37**, 911–917.
38 L. Ricci-Vitiani, D. G. Lombardi, E. Pilozzi, M. Biffoni, M. Todaro, C. Peschle and R. De Maria, *Nature*, 2007, **445**, 111–115.
39 D. Mizrak, M. Brittan and M. Alison, *J. Pathol.*, 2008, **214**, 3–9.
40 J. Miki and J. S. Rhim, *Prostate Cancer Prostatic Dis.*, 2008, **11**, 32–39.
41 S. Ma, T. K. Lee, B. J. Zheng, K. W. Chan and X. Y. Guan, *Oncogene*, 2008, **27**, 1749–1758.
42 W. Zhu, T. Hai, L. Ye and G. J. Cote, *J. Clin. Endocrinol. Metab.*, 2009, **95**, 439–444.
43 M. M. Bradford, *Anal. Biochem.*, 1976, **72**, 248–254.
44 G. R. Bartlett, *J. Biol. Chem.*, 1959, **234**, 466–468.
45 J. N. Israelachvili and D. J. Mitchell, *Biochim. Biophys. Acta*, 1975, **389**, 13–19.
46 D. Kirpotin, J. W. Park, K. Hong, S. Zalipsky, W. L. Li, P. Carter, C. C. Benz and D. Papahadjopoulos, *Biochemistry*, 1997, **36**, 66–75.
47 J. J. Vredenburgh, A. Desjardins, J. E. Herndon 2nd, J. M. Dowell, D. A. Reardon, J. A. Quinn, J. N. Rich, S. Sathornsumetee, S. Gururangan, M. Wagner, D. D. Bigner, A. H. Friedman and H. S. Friedman, *Clin. Cancer Res.*, 2007, **13**, 1253–1259.
48 Y. Matsumura and H. Maeda, *Cancer Res.*, 1986, **46**, 6387–6392.
49 K. Maruyama, T. Yuda, A. Okamoto, S. Kojima, A. Suginaka and M. Iwatsuru, *Biochim. Biophys. Acta*, 1992, **1128**, 44–49.
50 D. Liu, A. Mori and L. Huang, *Biochim. Biophys. Acta*, 1992, **1104**, 95–101.
51 T. Lian and R. J. Ho, *J. Pharmaceut. Sci.*, 2001, **90**, 667–680.